Model for Spiral Wave Formation in Excitable Media

Ehud Meron [a]
The James Franck Institute, The University of Chicago, Chicago, Illinois 60637
and
Pierre Pelcé
Laboratoire de Recherche en Combustion, Université de Provence, 13397 Marseille Cedex 13, France
(Received 30 November 1987)

A model for the velocity of a wave front having a free edge and moving in an excitable medium is proposed. It contains three main ingredients: a curvature effect, a normal velocity-profile effect at a free edge, and a finite-width effect. The model allows one to study the process in which arbitrary initial conditions evolve into rotating spiral waves. Two new scaling laws, for the time to form a spiral's core and for the distance between the cores of a mirror-image pair of rotating spiral waves, are numerically derived.

PACS numbers: 82.40.Fp, 87.90.+y

Rotating spiral waves are robust patterns in excitable media. They have been observed in chemically reactive solutions,[1] in the heart muscle,[2] in the human brain,[3] in the retina of the eye,[4] and in cultures of the social amoebas Dictyostelium discoideum.[5] Their beauty, the challenging difficulties that their analysis presents, and their physiological importance[2] have attracted enormous attention of both theorists[2,6-8] and experimentalists.[2,9-11] Though, in many respects, studies of spiral wave patterns have been successful, there still remain important unresolved questions. One of these concerns the dynamical process in which initial conditions develop into a spiral structure. As yet, the physical principles and the dynamical laws which govern this process have not been satisfactorily traced.

In this Letter, we propose a model for the velocity of a wave front having two free edges and moving in an excitable medium. Three principal physical ingredients are taken into account: a diffusion-induced curvature effect, a normal velocity-profile effect at a free edge induced by tangential diffusion, and a wave-width effect. The model allows us, in the first place, to propagate quite arbitrary initial conditions into rotating spiral wave patterns, and thus to demonstrate the process of spiral wave formation. The model is further used to derive new scaling relations between experimentally observable quantities. More specifically, we find that the time t_c to form a spiral's core scales like the excitation rise time τ, and is independent of the diffusion constant D, the rehabilitation time T, and the length of the initial wave front, L. We also find that the distance R between the two cores of a mirror-image pair of rotating spiral waves follows an exponential law of the form $R/L=\exp[A(v)u^{\alpha}]$, where $u=D\tau/L^2$, $\alpha\cong 0.49$, and $A(v)$ is an undetermined function of $v=T/\tau$.

"Excitable media" is a generic name for spatially extended systems in a stable steady state which are, however, susceptible to small perturbations. Consider, for the sake of illustration, the following simple example of excitable kinetics[12]:

$$\epsilon\dot{c}_1=-c_2+3c_1-c_1^3, \tag{1a}$$

$$\dot{c}_2=c_1-\delta, \tag{1b}$$

where ϵ is a small parameter and the overdot denotes derivation with respect to time. The phase space of Eqs. (1) contains a "slow manifold" defined by the nullcline $c_2=3c_1-c_1^3$, and a fixed point S at $(c_1,c_2)=(\delta,3\delta-\delta^3)$. The fixed point is stable (unstable) for $|\delta|>1$ ($|\delta|<1$). Suppose that S is stable and lies close to the minimum of the slow manifold, as illustrated in Fig. 1(a). Consider now two points A and B in the vicinity of S such that the vector field of Eqs. (1) points towards S and away from S, respectively [see Fig. 1(a)]. A system in S which is perturbed to A immediately relaxes back to S. However, when it is perturbed to B a long excursion

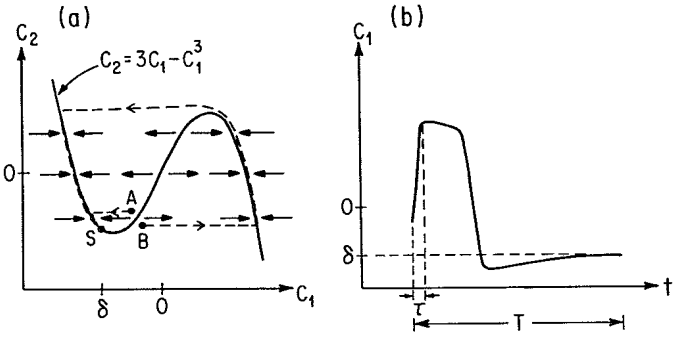

FIG. 1. (a) Phase space for Eqs. (1) and (b) time signal of the fast variable, c_1, after excitation. The system evolves slowly along the stable branches of the slow manifold. When it is forced to leave the slow manifold, fast relaxation back to a stable branch occurs. For more details see text.

in phase space, independent of the exact location of B, takes place before relaxation back to S occurs. A typical time signal of the fast variable, $c_1(t)$, when the threshold of excitation is exceeded is shown in Fig. 1(b). Notice that after excitation the system spends a long time along the left branch of the slow manifold ($c_1 < \delta$) where it is not susceptible to small perturbations; we say that the system is in its *refractory period.* We use then name "rehabilitation time" to denote the total duration, T, of the excursion in phase space after excitation.

The combination of excitability and diffusive coupling between adjacent volume elements gives rise to a variety of traveling-wave patterns.[1,2] A characteristic feature of excitable media is that any wave front is followed by a refractory tail in which the medium is not reexcitable. The width of the refractory tail is determined by the refractory period and the front velocity. In two-dimensional systems the most stable patterns are rotating spiral waves. They form whenever a free edge of a propagating wave front is created (hereafter an "open front"). Open fronts are generally created by nonuniformities in the medium: dispersion of refractory times, phase gradients, impurities in chemical solutions, etc.

Consider now an open wave front whose position vector is $\mathbf{X}(s,t)$, where s and t are, respectively, arc length and time, as illustrated in Fig. 2. The velocity of the front can be written as

$$d\mathbf{X}/dt = U\hat{\mathbf{r}} + \sigma\hat{\mathbf{s}}, \tag{2}$$

where $\hat{\mathbf{r}}$ and $\hat{\mathbf{s}}$ are, respectively, the normal and tangent unit vectors. We will assume that the tangential velocity at the free edges of the front is independent of time. For the normal velocity we propose the following form:

$$U = c + \frac{a\kappa}{1 - w\kappa} - b\left[\exp\left(-\frac{s}{d}\right) + \exp\left(-\frac{l(t)-s}{d}\right)\right]. \tag{3}$$

Here, c is the velocity of a planar wave front away from an edge point, $\kappa(s,t)$ is the curvature (by convention, negative for convex fronts), w is a measure of the wave's width, and $l(t)$ is the wave front's length.

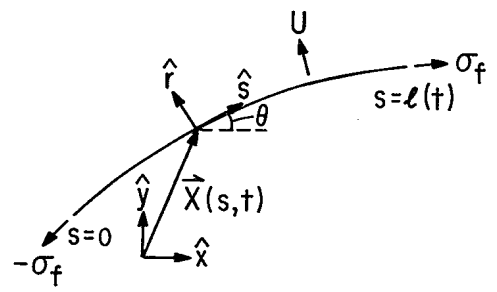

FIG. 2. Schematic illustration of an open front described by a position vector $\mathbf{X}(s,t)$ and moving with a normal velocity $U(s,t)$ and constant tip tangential velocity σ_f.

The model is based on the following physical understanding. Diffusion acts to reduce (enhance) the normal velocity of a convex (concave) wave front with respect to the velocity of a planar wave front, and thus to stabilize the front against small-wavelength perturbations. This stems from the observation that a convex (concave) geometry reduces (enhances) the diffusion flux into an area element ahead of the front and, consequently, a longer (shorter) time is required for the diffusion process to exceed the excitation threshold in that area element. For the same reason, tangential diffusion at a free edge of the front induces a normal velocity profile which imposes on the free edge a persistent bias to curl. The curvature at the tip eventually saturates because of a finite-width effect: The wave front is followed by a refractory tail consisting of sites which are not reexcitable. When the tip starts probing these sites curvature saturation begins. A schematic illustration of these physical effects is shown in Fig. 3. The numerator of the second term in the right-hand side of Eq. (3) models the diffusion-induced stabilizing effect described above. The parameter a is positive and has the dimension of a diffusion constant. The third term represents a simple modeling of the velocity profiles at the two free edges, while the denominator of the second term models, in a local manner, the finite-width effect (see discussion below). We note that for small curvature and away from an edge point, Eq. (3) reduces to $U = c + a\kappa$. Such an expression can be rigorously derived from the original reaction-diffusion equations.[8,13]

Instead of solving Eq. (2) for $\mathbf{x}(s,t)$, we found it convenient to derive first a partial differential equation for the curvature of the wave front. Once the curvature field $\kappa(s,t)$ is known the curve $\mathbf{X}(s,t)$ can be constructed. The equation for the curvature is derived in the spirit of Brower *et al.*[14] Since the tangential velocity σ is varying between time-independent limits, $\sigma(s=0) \equiv -\sigma_f$ and $\sigma(s=l) \equiv +\sigma_f$, it is convenient to reparametrize the curve $\mathbf{X}(s,t)$ by σ. To this end we introduce the metric

$$h(\sigma,t) = (\mathbf{q}\cdot\mathbf{q})^{1/2}, \quad \mathbf{q} \equiv \frac{\partial \mathbf{X}}{\partial \sigma} = \frac{\partial s}{\partial \sigma}\hat{\mathbf{s}}, \tag{4}$$

in terms of which the arc length is given by

$$s(\sigma,t) = \int_{-\sigma_f}^{\sigma} h(\sigma',t)\,d\sigma'. \tag{5}$$

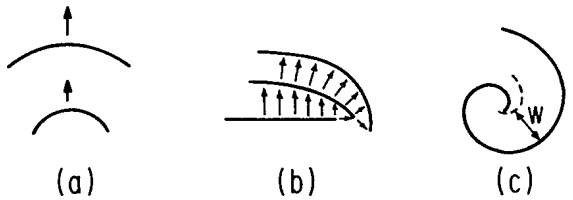

FIG. 3. (a) Schematic illustration of the curvature effect, (b) the normal velocity-profile effect at a free edge, and (c) the finite-width effect. The arrows indicate velocity vectors.

We need now two equations for the two unknowns $\kappa(\sigma,t)$ and $h(\sigma,t)$. Considering the two-dimensional space as the complex plane $z=x+iy$, we write

$$q=\partial z/\partial\sigma=h\exp(i\theta),\quad r=i\exp(i\theta),\tag{6}$$

where $\theta(\sigma,t)$ is the angle between the tangent vector and a fixed direction chosen to be the x axis (see Fig. 2). Taking now the time derivatives of q once according to Eq. (6) and once according to Eqs. (4) and (2) and using the curvature definition, $\kappa\equiv\partial\theta/\partial s$, we find

$$\partial h/\partial t=1-hU\kappa,\tag{7a}$$

$$\frac{\partial\kappa}{\partial t}=\left(\kappa^2+\frac{1}{h^2}\frac{\partial^2}{\partial\sigma^2}\right)U+\frac{\sigma}{h}\frac{\partial\kappa}{\partial\sigma}-\frac{1}{h^3}\frac{\partial U}{\partial\sigma}\frac{\partial h}{\partial\sigma}.\tag{7b}$$

We solve Eqs. (7) numerically using the Cranck-Nicholson scheme.[15] Figure 4 shows the time evolution of a straight line. Symmetric initial conditions lead to a symmetric pattern consisting of a mirror-image pair of rotating spiral waves.

In order to relate the model to physical systems we resort to dimensional analysis. Four important physical parameters determine the dynamics and the structure of the spiral wave (with the assumption that the initial conditions are in the form of a straight line): L, τ, D, and T. Of these, only two have independent dimensions. The time t_c to form a core and the distance R between the two cores of a symmetric pattern can therefore be written as

$$t_c=\tau f(u,v),\quad R=Lg(u,v),\tag{8}$$

where $u\equiv D\tau/L^2$ and $v\equiv T/\tau$ are dimensionless variables. The functions f and g can be evaluated by numerical integration of Eqs. (7) once the relations between the model parameters and the parameters L, τ, D, and T are known. These are obtained by dimensional considerations: c, b, $\sigma_f\sim(D/\tau)^{1/2}$, $a\sim D$, $d\sim(D\tau)^{1/2}$, and $w\sim T(D/\tau)^{1/2}$.

For the evaluation of $f(u,v)$ we define t_c as the time required to form a pattern similar to the third from top shown in Fig. 4 (the results are insensitive to the exact definition of t_c). We find that within an error of less than a percent $f(u,v)$ is a constant function. Different u,v values lead to quite distinctive patterns, yet t_c/τ remains the same. The distance R between the two cores of a symmetric pattern is evaluated by our measuring the horizontal coordinate of the spiral tip at two successive patterns in Fig. 4 (third and fourth from top, for example) and taking the mean value. Figure 5 shows a plot of $\ln[\ln(g)]$ vs $\ln(u)$ at a constant v value. The numerical data suggest the law $g=\exp[A(v)u^{\alpha}]$ where $\alpha\cong0.49$ and A is some (undetermined yet) function of v. Notice that for large patterns ($u\to0$) $R/L\to1$. The parameters L and τ can be controlled in a continuously fed unstirred reactor type experiment.[16] Thus the predicted forms of both f and g can be tested experimentally.

The model presented above is local. When the curvature at the tip saturates on a value which is comparable to or larger than w^{-1}, nonlocal effects become important: The tip velocity is affected by the recovery rate of sites which belonged to the front at earlier times and were located at different arc-length values. We note, however, that properties such as t_c and R are determined by the early stages of the spiral wave evolution and therefore are not sensitive to these nonlocal effects. Asymptotic properties, on the other hand, such as the spiral wavelength, should be treated with caution.[17]

We wish to thank Leo Kadanoff and Albert Libchaber for encouraging us to study this problem and for some fruitful conversations. Useful discussions with Harry

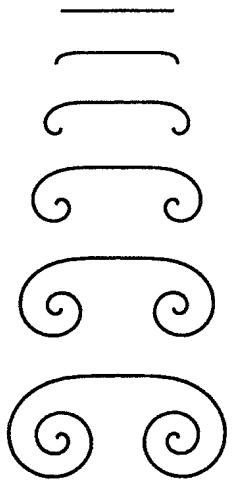

FIG. 4. Time evolution of a straight front having two free edges.

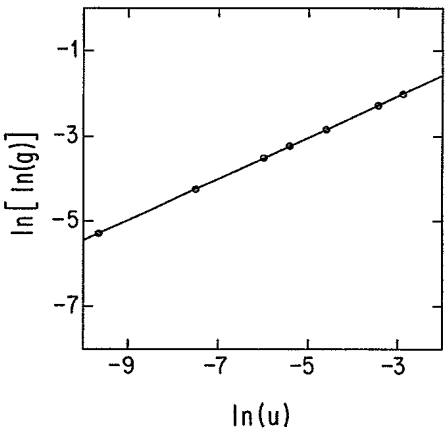

FIG. 5. Numerical data for the function $g(u,v)=R(u,v)/L$ taken at a constant v value. The solid line is a best fit of the data by a straight line. The slope of the line gives the exponent α.

Swinney, Wing Tam, Pierre Coullet, and Oreste Piro are acknowledged as well. This study has been supported by the Material Research Laboratory at the University of Chicago and by the Chaim Weizmann Foundation.

---

[a]Present address: Astronomy Department, Columbia University, New York, NY 10027.

[1]R. J. Field and M. Burger, *Oscillations and Traveling Waves in Chemical Systems* (Wiley, New York, 1985).

[2]A. T. Winfree, *When Time Breaks Down* (Princeton Univ. Press, Princeton, New Jersey, 1987).

[3]M. Shibata and J. Bures, J. Neurobiol. **5**, 107 (1974).

[4]N. A. Gorelova and J. Burnes, J. Neurobiol. **14**, 353 (1983).

[5]W. F. Loomis, *The Development of Dictyostelium Discoideum* (Academic, New York, 1982).

[6]A. S. Mikhailov and V. I. Krinsky, Physica (Amsterdam) **9D**, 346 (1983).

[7]P. C. Fife, J. Stat. Phys. **39**, 687 (1985).

[8]J. P. Keener and J. J. Tyson, Physica (Amsterdam) **21D**, 307 (1986).

[9]H.-G. Busse, J. Phys. Chem. **73**, 750 (1969).

[10]A. N. Zaikin and A. M. Zhabotinskii, Nature (London) **225**, 535 (1970).

[11]S. C. Muller, T. Plesser, and B. Hess, Physica (Amsterdam) **24D**, 71,87 (1987).

[12]J. Cronin, *Mathematical Aspects of Hodgkin-Huxley Neural Theory* (Cambridge Univ. Press, New York, 1987).

[13]M. L. Frankel and G. I. Sivashinsky, J. Phys. (Paris) **48**, 25 (1987).

[14]R. C. Brower, D. A. Kessler, J. Koplik, and H. Levine, Phys. Rev. Lett. **51**, 1111 (1983), and Phys. Rev. A **29**, 1335 (1984).

[15]W. H. Press, B. P. Flannery, S. A. Teukolsky, and W. T. Vetterling, *Numerical Recipes* (Cambridge Univ. Press, New York, 1986).

[16]W. Y. Tam, W. Horsthemke, Z. Noszticzius, and H. L. Swinney, to be published.

[17]Notice that nonlocal effects due to diffusion do not arise at the early stages of the spiral wave evolution: The radius of curvature κ^{-1} is bounded from below by a number of $O(w)$ while $w \sim T(D/\tau)^{1/2}$ is much larger than the diffusion length $(D\tau)^{1/2}$.